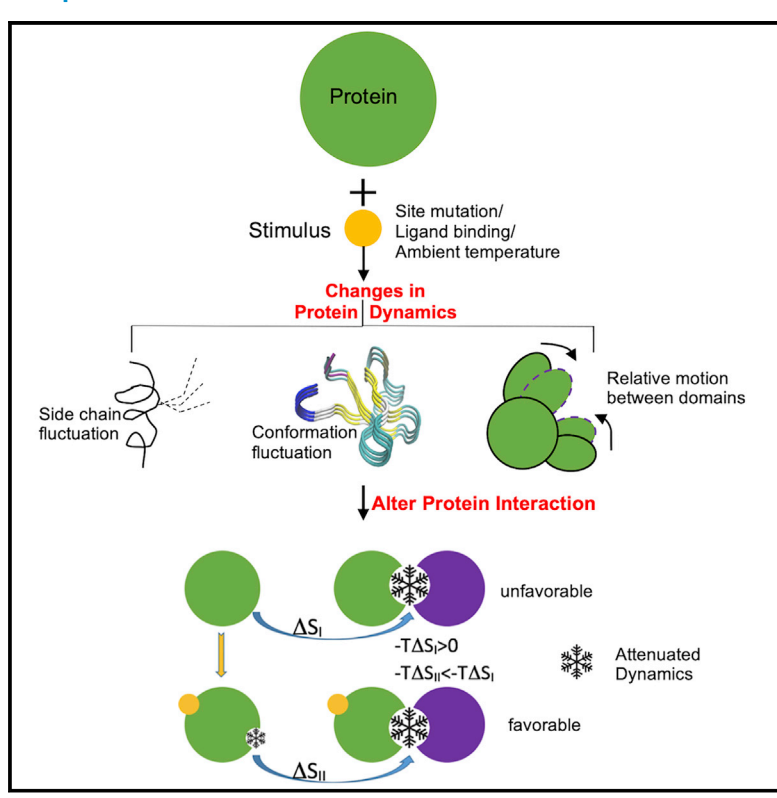
# Computational studies of the principle of dynamicchange-driven protein interactions

# **Graphical abstract**



## **Authors**

Zhen-lu Li, Carla Mattos, Matthias Buck

# Correspondence

zhenlu.li@tju.edu.cn (Z.-l.L.), matthias.buck@case.edu (M.B.)

# In brief

Li et al. provide evidence of dynamic allostery and entropy-driven protein association. Quantitative entropy calculations demonstrate that formation of the Ras homodimer is triggered by the effector protein Raf RBD, which attenuates the internal fluctuations in Ras and reduces unfavorable entropy prior to binding.

# **Highlights**

- Allostery associated with dynamic changes regulates protein recognition and function
- RBD enhances RAS-RAS association by reducing the entropy penalty for dimer formation
- Conformational plasticity of ADK affects protein collective modes and substrate binding
- Quenching of protein internal dynamics stimulates the SAM-SAM protein interaction







# **Theory**

# Computational studies of the principle of dynamic-change-driven protein interactions

Zhen-lu Li,1,2,\* Carla Mattos,3 and Matthias Buck1,4,5,6,\*

<sup>1</sup>Department of Physiology and Biophysics, School of Medicine, Case Western Reserve University, 10900 Euclid Avenue, Cleveland, OH 44106, USA

<sup>2</sup>School of Life Science, Tianjin University, Tianjin 300072, China

<sup>3</sup>Department of Chemistry and Chemical Biology, Northeastern University, 360 Huntington Avenue, Boston, MA 02115, USA

<sup>4</sup>Department of Pharmacology, School of Medicine, Case Western Reserve University, 10900 Euclid Avenue, Cleveland, OH 44106, USA

<sup>5</sup>Department of Neurosciences, School of Medicine, Case Western Reserve University, 10900 Euclid Avenue, Cleveland, OH 44106, USA

\*Correspondence: zhenlu.li@tju.edu.cn (Z.-l.L.), matthias.buck@case.edu (M.B.) https://doi.org/10.1016/j.str.2022.03.008

#### **SUMMARY**

Dynamic allostery emphasizes a role of entropy change manifested as a sole change in protein fluctuations without structural changes. This kind of entropy-driven effect remains largely understudied. The most significant examples involve protein-ligand interactions, leaving protein-protein interactions, which are critical in signaling and other cellular events, largely unexplored. Here we study an example of how protein-protein interaction (binding of Ras to the Ras binding domain [RBD] of the effector protein Raf) affects a subsequent protein association process (Ras dimerization) by quenching Ras internal motions through dynamic allostery. We also investigate the influence of point mutations or ambient temperature, respectively, on the protein dynamics and interaction of two other systems: in adenylate kinase (ADK) and in the EphA2 SAM:Ship2 SAM complex. Based on these examples, we postulate that there are different ways in which dynamic-change-driven protein interactions are manifested and that it is likely a general biological phenomenon.

#### **INTRODUCTION**

Allostery is a process by which proteins transmit the effect of binding at a primary site to a secondary site, triggering protein structural and/or dynamic changes and affecting functional activity. The changes in protein structure may be a global protein configurational transition or local displacement of a protein residue or a secondary structural element (loop, helix,  $\beta$  sheet). Visualization of these changes in structures has long been a focus in structure determination by X-ray crystallography and, more recently, by high-resolution cryoelectron microscopy (cryo-EM). Ligand binding and residue mutation are common triggering factors for protein allostery. Well-known examples include allostery of transmembrane helices in G protein-coupled receptors (GPCRs) or in membrane transporters upon ligand binding (Ranade et al., 2015). For enzyme catalysis, allostery usually involves a more complicated structure change process at multiple levels, involving side-chain recognition, loop displacement, and relative movements between domains (Lisi and Loria, 2017; Papaleo et al., 2011).

Changes in a protein can also occur at a second site in response to change at a primary site by manifesting as merely an alteration of protein dynamics without a significant conformational change. This process is called dynamic allostery. Dynamic allostery distinguishes itself from the wider concept of allostery (structure-based allostery). It emphasizes a role of entropy

change at a protein site, which is apparent by altered local thermal fluctuations of the amino acid constituent atoms around their average positions in the protein's structure. Protein dynamic allostery was originally proposed 38 years ago (Cooper and Dryden, 1984). Despite its importance, dynamic allostery mechanisms, in most instances, remain largely understudied because of computationally or experimentally technical difficulties. Complex multicomponent signaling systems are particularly challenging to study in terms of allostery, and theoretical and experimental validation of dynamic allostery in the general protein signaling process has yet to be done. Characterization of the fluctuations of individual amino acid atoms in a protein only became possible with the advent of sophisticated experiments using nuclear magnetic resonance (NMR) and more extensive molecular dynamics (MD) simulations capabilities developed in the 2000s and 2010s (Grutsch et al., 2016; Strotz et al., 2020; Zhang et al., 2012). Extensive studies via NMR or MD simulations have been carried out to characterize how a ligand binding or amino acid mutation event may spread to a distal region of a protein and lead to changes in local atom/residues fluctuations via one or more allosteric networks (Ahuja et al., 2019; Bouguet-Bonnet and Buck, 2008; Chakrabarti et al., 2020; Henzler-Wildman et al., 2007; Koss et al., 2018; Petit et al., 2009; Weinkam et al., 2013; Zerbetto et al., 2013; Zhang and Buck, 2017). It is relatively easy to characterize the dynamic change of a protein caused by an external stimulus, but it is more challenging to







assess, if not quantify, how the changes in residue fluctuations may affect downstream protein functional processes such as protein association, signaling, or catalysis.

To date, the essential role of dynamic allostery in modulating a successive protein event is understood only in a few cases (Arora and Brooks, 2007; Barman and Hamelberg, 2016; Kaplan et al., 2016; Popovych et al., 2006; Saavedra et al., 2018; Tzeng and Kalodimos, 2009; Feng et al., 2018). The first example of dynamic-allostery-driven substrate association was cooperative binding of Ca<sup>2+</sup> to Calbindin D9k (Akke et al., 1993a, 1993b). NMR relaxation data showed that binding of a first cationic ion to Calbindin attenuates the intramolecular fluctuations of the protein. The decrease in protein fluctuations enhances binding of a second cationic ion because of a reduced entropy penalty. Catabolite activator protein (CAP) is a relatively well-characterized protein that serves as another example of how the dynamic change caused by the first ligand binding event can dramatically affect the second ligand binding. Here, binding the first cyclic AMP (cAMP) to the protein CAP gives an entropy penalty of -3.2 kcal/mol. However, the second cAMP binding needs to pay a much higher entropy penalty of -18.1 kcal/mol, largely because of the dynamic changes caused by the first cAMP binding (Popovych et al., 2006; Tzeng and Kalodimos, 2009). For both situations, effects of dynamic-allostery-driven substrate associations were observed in the binding process of a protein when a first binding event is followed by a second small ion or small ligand interaction. In these cases, measurement of dynamic changes could be focused on one protein. For dynamic allostery processes involving multiple proteins, a comprehensive description can be more challenging.

Processes that are merely driven by entropy changes without conformational changes are the best systems for studying protein dynamic allostery. In nature, these systems have been difficult to detect with existing tools and appear to be rare. In most cases studied in detail, changes in dynamics are mixed with structural changes, which makes it hard to discern the thermodynamic role of protein entropy, caused by a change in residue fluctuations alone. In this study, we explore the role of dynamic allostery on regulating protein interaction in three systems. Each example represents inherently different entropically driven processes because of allosteric events without changes in the average conformations of the proteins: (1) Raf-Ras binding domain (RBD)-driven Ras dimerization (Cookis and Mattos, 2021; Packer et al., 2021), (2) enhanced adenylate kinase (ADK) catalysis because of elevated protein dynamics as a result of point mutations (Saavedra et al., 2018), and (3) enhanced complex formation between the SAM domains of EphA2 and Ship2 at decreased temperatures (Lee et al., 2012). Here we visit these three cases with an emphasis on entropy analysis, which clearly shows the effects of dynamic allostery critical for the emerging principle of dynamic-change-driven protein interactions (DCDPI).

#### **RESULTS**

#### **RBD-driven Ras dimerization**

Recently, a process of Ras dimerization stimulated by the C-Raf RBD was identified (Cookis and Mattos, 2021; Packer et al., 2021). Ras is a small GTPase that, by itself, is monomeric in so-

lution (Kovrigina et al., 2015) and on membranes (Chung et al., 2018). In the presence of the C-Raf RBD, however, it forms a dimer with a  $K_d$  estimated to be 37  $\mu$  M on supported lipid bilayers (Packer et al., 2021). In this report, we show that K-Ras dimerization is predominantly an entropy-driven effect, associated with an allosteric dynamic change stimulated by RBD binding. This premise is supported by the observation that the association with the RBD has little visible influence on the Ras structure. The root-mean-square deviation (RMSD) is 0.48 Å for the catalytic domain of residues 1-166, comparing the K-Ras homologous H-Ras in complex with the RBD (PDB: 4G0N) with the free GTPase (PDB: 3K8Y). In particular, the RBD:K-Ras interface is highly similar to the RBD: H-Ras interface (PDB: 7JHP) with a RMSD of 0.19 Å for the allosteric lobe of residues 86-166 compared with H-Ras in PDB: 7JHP, where the Ras:Raf complex appears as a monomer with the RBD:Ras 2:2 dimer present in crystals with PDB: 4G0N. Using this protein complex as a model system, we investigate the influence of dynamic allostery triggered by RBD association on formation of the Ras dimer.

Computationally, we consider two processes for the monomer-homodimer transition: K-Ras4B homodimerization by itself (process I,  $\Delta S_I$ ) and K-Ras4B homodimer formation following K-Ras binding of the RBD (process II,  $\Delta S_{II}$ ) (Figure 1A). Specifically, we simulated free K-Ras4B, the bound K-Ras4B dimer, the bound K-Ras4B:RBD complex, and the 2:2 RBD-K-Ras4B:K-Ras4B-RBD complex. We carried out MD simulations on each set of systems with at least 4 replicates with a total simulation time of 13 µs using the CHARMM36m potential function (Table S1). Given that the protein-protein interaction interfaces in K-Ras4B dimerization are the same with and without RBDs on the opposite end of the complex, we make the reasonable approximation that the enthalpy contribution in the free energy change associated with process I and process II is the same and thus the enthalpy difference between these processes is negligible. Therefore, the entropy difference ( $\Delta\Delta S$  =  $\Delta S_{II} - \Delta S_{I}$ ) between the two processes reflects the dominant part of the free energy difference. Full results for entropy values of proteins for different time intervals and different replicas are listed in Table S2. The mean entropy values of K-Ras4B and RBD are summarized in Figure 1B. As shown in Figure 1B, formation of the K-Ras dimer by itself from K-Ras monomers is at the cost of conformational entropy ( $\Delta S_1 = -0.15 \text{ kcal/mol/K}$ ,  $-T\Delta S_{I}$  = 46.5 kcal/mol); however, with the effector Raf RBD bound, the entropy penalty of K-Ras4B is reduced to -0.05 kcal/mol/K. There is also a small gain of entropy of 0.02 kcal/mol/K for the RBD in process II, but this contribution of the RBD lacks statistical significance because of its small magnitude. Therefore, the major source of entropy penalty is K-Ras4B. This results in a net loss of entropy for process II of -TΔS<sub>II</sub> of 15.5 kcal/mol. Thus, K-Ras4B has an enhanced tendency to form a dimer in the presence of the C-Raf RBD. As further evidence of this entropy-driven effect, we performed two sets of short simulations of 200 ns each with a different force field: the Amber potential function (ff19SB). The results showed that the entropy penalty for K-Ras4B dimerization from the free proteins was 34.3 kcal/mol. With the aid of the bound RBD, however, the entropy penalty was reduced to 10.5 kcal/mol (Table S3). Despite the brief simulation time, it



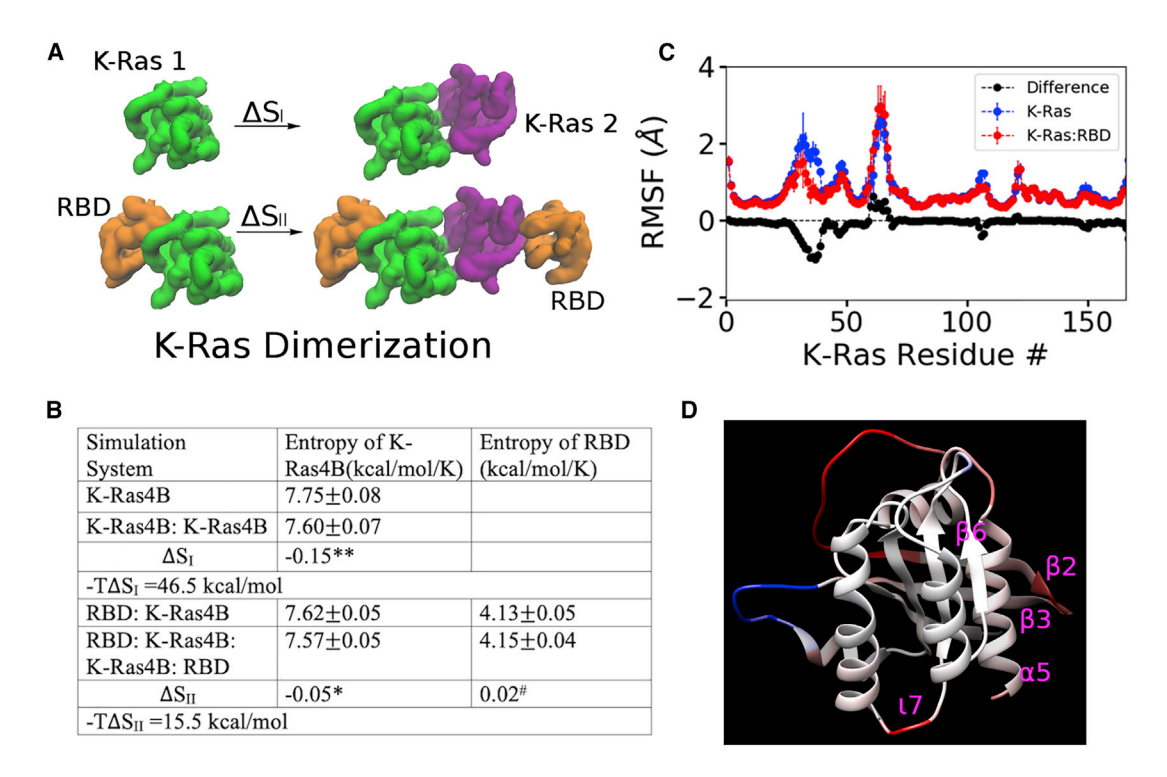


Figure 1. RBD stimulated K-Ras dimerization

(A) The monomer-homodimer transition of K-Ras4B (green and purple) by itself (process I) and K-Ras4B:RBD (orange) as a 2:2 complex (process II). (B) Entropy change in a monomer-homodimer transition of K-Ras4B by itself (process I) and K-Ras4B:RBD as a complex (process II). Statistical significance: #p > 0.05, \*p < 0.01, \*\*p < 0.001. See also Tables S2 and S3.

- (C) Quenching of protein internal dynamics of K-Ras4B caused by RBD association, shown by a difference in RMSF (see also Figure S1).
- (D) Mapping of the RMSF difference (ΔRMSF) on the K-Ras4B structure. Color ranges from red (ΔRMSF ≤ −0.4 Å) to blue (ΔRMSF ≥ 0.4 Å).

shows a consistent trend where the RBD association reduces the entropy penalty for K-Ras4B dimerization.

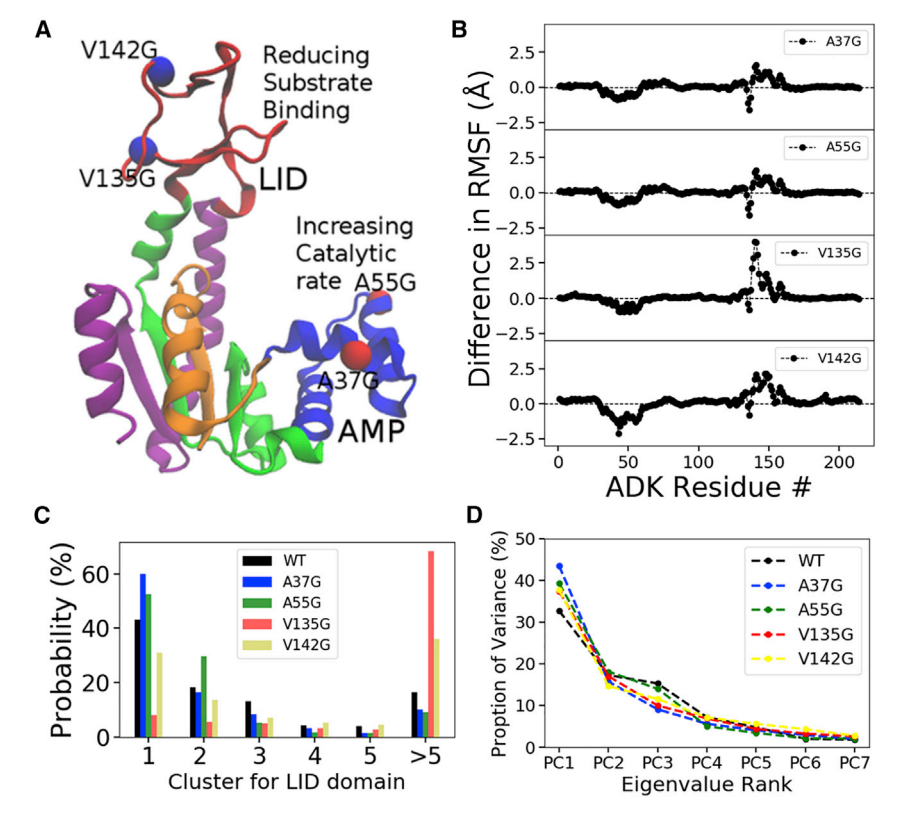
The K-Ras: RBD interface involves switch I (res. 26-37) and the N-terminal part of  $\beta$ 2 (res. 38–46). The K-Ras:K-Ras dimerization interface involves the  $\beta$ 2- $\beta$ 3 loop (res. 46–49) and  $\alpha$ 4- $\beta$ 6- $\alpha$ 5 (res. 127-165). Figures 1C and 1D show that, upon RBD binding, the fluctuations are largely reduced for the entire switch I and the first few residues of  $\beta 2$  (res. 38, 49, 40). In contrast, switch II (res. 58– 65) has increased fluctuations. At the K-Ras dimerization interface, the  $\beta$ 2- $\beta$ 3 loop (res. 46-49) and the loop connecting  $\beta$ 6 and α5 (res. 145–151) experience an obvious reduction in rootmean-square fluctuation (RMSF) (Figures 1C and 1D). The fluctuation of loop 7 (res. 105-109), which is in the vicinity of the Ras dimerization interface, is also repressed. The fluctuation information indicates that RBD binding largely represses the fluctuation at RBD:K-Ras4B binding interface regions. Importantly, the repression of protein fluctuations goes beyond the RBD:K-Ras4B interface and has an effect at other regions, including the K-Ras4B dimerization interface and neighboring regions (Figure 1D). Therefore, there is a diminished need for further rigidification in the transition from the 1:1 RBD:K-Ras4B complex to a 2:2 complex upon dimerization via K-Ras (Figure S1), and, consequently, there is a reduced entropy penalty. Previous MD simulations of H-Ras and a Raf-RBD and of the H-Ras:RBD complex show selective rigidification of key functional areas in Ras, including areas of helices 4 and 5 involved in dimerization as well as global rigidification of the RBD upon complex formation (Fetics et al., 2015). This is in line with our current results for K-Ras. It is clear that the entropic cost for Ras dimerization is paid largely in advance by formation of the high-affinity Ras:RBD complex, driven by extensive enthalpic interactions at the complex interface involving multiple salt bridges (Fetics et al., 2015; Li and Buck, 2019). In summary, RBD-stimulated Ras dimerization is a highly suitable example for a protein association event predominantly driven by the entropy effect because of dynamic allostery.

# ADK catalysis is influenced by a point mutation altering protein dynamics

Next we investigate the role of local dynamic changes on the conformation and dynamics of an entire protein (ADK) and revisit its potential role in regulating substrate binding and catalysis. ADK catalyzes reversible phosphoryl transfer from ATP to AMP to yield two molecules of ADP, and it is commonly used to study the connections between enzyme catalysis and protein allostery (Saavedra et al., 2018). The dynamics of this enzyme are more complicated than the Ras dimerization process studied above. To achieve catalysis, the ADK molecule undergoes a significant structural/conformational transition between an inactive "open" state and an active "closed" state. The conformational transition involves relative movement between the LID domain and AMP domain. The LID domain is responsible for initial binding with a substrate molecule. Catalysis is completed when the LID domain brings the substrate close to the AMP domain. It has been shown







that certain point mutants can dramatically affect catalysis of ADK via a dynamic allostery process (Saavedra et al., 2018). Remarkably, the site mutations do not alter the average conformation of a domain (LID or AMP) but affect the fluctuations of the domain (dynamic allostery). This affects substrate binding and the rate of relative motions between domains (LID and AMP domains). Specifically, a point mutation in the LID domain (V135G or V142G) weakens substrate binding (an increase in K<sub>M</sub> in kinetics experiments) and has moderate influence on catalytic efficiency. Point mutations in the AMP domain (A37G or A55G) have less influence on substrate binding but largely increase the catalytic rates.

To gain additional atomistic details for the inherent mechanism of dynamic allostery associated with ADK, we carried out a set of simulations (in duplicate) totaling 5  $\mu$ s for wild-type ADK and for four ADK mutants in their inactive state (Figure 2A; Table S1). The mutation V135G or V142G in the LID domain increases the main-chain fluctuations (RMSF) of the protein (Figures 2B and S2A) and considerably increases the conformational flexibility of the LID domain (Figure 2C) because there are more conformations that deviate from the average conformation (cluster > 5) with these two mutations. The reaction process involves structural and dynamic changes at multiple levels, such as substrate association and release, and relative domain movement between the LID and AMP domains. We are therefore not able to build a free energy cycle for ligand-protein binding as done for Ras and its RBD binding partner. The opposite effect to quenching of protein internal dynamics (i.e., an increase in protein internal dynamics, also known as tempering) would attenuate the protein:ligand association. We infer that the increased protein fluctuation would weaken LID:substrate binding. Mutation of Ala37 to Gly or Ala55 to Gly in

Figure 2. Influence of point mutations on ADK protein dynamics

(A) ADK structures in the open state. The segments of the N terminus (1-29, orange), AMP (30-73, blue), hinge (74-121, green), LID (122-159, red), and C terminus (160-214, purple) are shown in different

- (B) Protein conformational flexibility for wild-type ADK and ADK mutants and plot of the difference in RMSF between wild-type ADK and ADK mutants.
- (C) Conformational clustering for the ADK LID
- (D) Principal-component analysis (PCA) of ADK and ADK mutants: the proportion of variance versus eigenvalue rank (see also Figure S2).

the AMP domain has less influence on the protein's flexibility (RMSF; Figure 2B) and does not increase deviation from the average structure for the LID domain (Figure 2C; conformational clustering for the ADK LID domain) or AMP domain (Figure S2B; conformational clustering for the ADK AMP domain); thus, there is little influence expected on substrate binding.

A collective mode analysis on the trajectories indicates that the proportion of soft modes, PC1 and PC2, are increased, in particularly for mutations Ala37 to Gly and Ala55 to Gly (Figures 2D and S2C). PC1 re-

ports relative motions that approach the center of the AMP and LID domains, similar to those that appear in a catalytic process, whereas PC2 indicates crisscross motions (Figure S2D). Both modes are relevant for the process of catalysis. Thus, we expect that the increased possibility of relative motions between AMP and LID could relate to the better performance of A37G or A55G mutations on increasing catalytic efficiency. These softened hinge motions and relevant collective motions may speed up the transition rates in a catalytic reaction. Similar to the case of RBD:K-Ras4B association, both sets of ADK mutations cause non-local perturbations. Residue-residue correlation maps indicate a moderate negative correlation between the LID and AMP domains (Figure S2E). The residue pair with the strongest correlation is established between A55 in the AMP domain and T155 in the LID domain. Allosteric pathways between the two residues are established, with several crucial connecting residues between the LID and AMP domains (Figure S2F). Thus, a site mutation effect in the AMP or LID domain could transmit to the distal LID or AMP, respectively. Each mutation, especially A37G and A55G, triggers a global change in protein plasticity (i.e., the soft modes PC1 and PC2; Figure 2D) associated with the mechanism of dynamic allostery that leads to enhanced catalysis.

In summary, the ADK analysis indicates that a point mutation may largely elevate the amplitude of conformational fluctuations of a protein at the local level. This is exemplified by the V135G and V142F point mutants of ADK, where fluctuations increase in the LID domain without changing the average conformation of the domain. This reduces the chance of substrate binding to the domain. On the other hand, a single-point mutant can also alter the global plasticity of the entire protein, again without



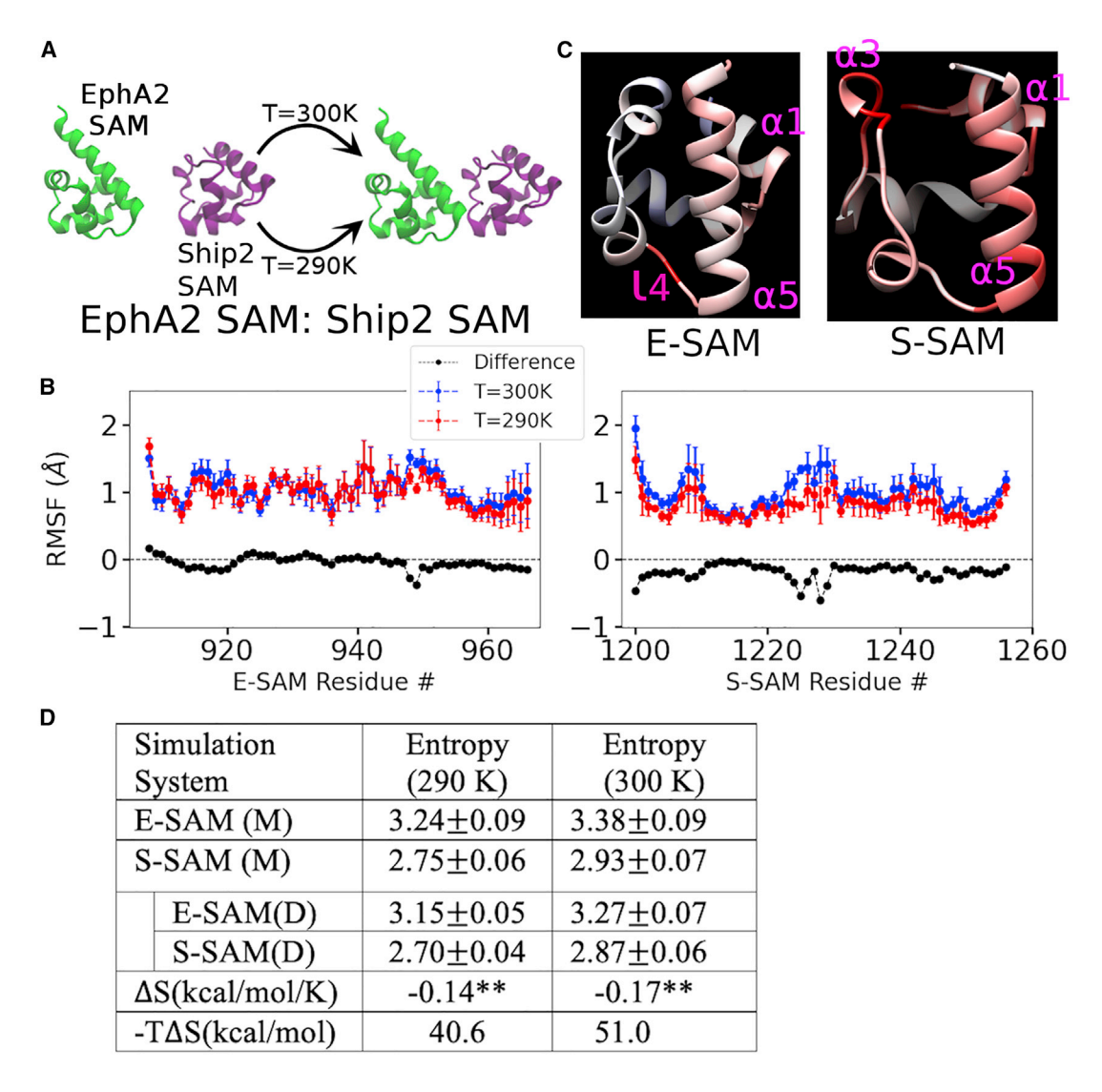


Figure 3. Influence of temperature on protein internal dynamics and protein interaction

(A) EphA2 SAM/E-SAM (green):SHIP2 SAM/S-SAM (purple) heterodimer formation at two different temperatures (300 K and 290 (K). (B) Quenching of protein internal dynamics for E-SAM and S-SAM because of the decrease in temperature (see also Figure S3). (C) Mapping of  $\triangle$ RMSF on E-SAM or S-SAM structure. Color ranges from red ( $\triangle$ RMSF  $\leq -0.4$  Å) to blue ( $\triangle$  RMSF  $\geq 0.4$  Å). Statistical significance: \*\*p < 0.001. (D) Entropy change in E-SAM:S-SAM heterodimer formation (D) at 300 K (blue) and 290 K (red) compared with SAM monomers (M) (difference in black) (see also Table S4).

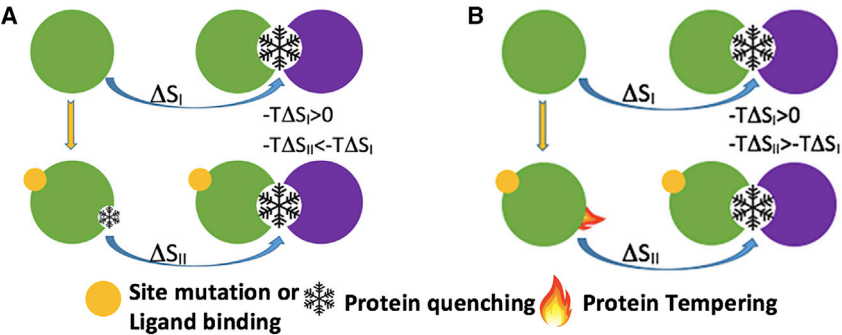
changing the average structure of the protein. In this case, it could heavily influence the kinetics of collective motion modes within the protein. This is exemplified by the ADK A37G or A55G point mutants, where the increased relative domain movements between the LID and AMP domains lead to increased catalytic efficiency. The ADK mutants show clearly how the functional outcome can be modulated by dynamic allostery in specific ways, and this can be a factor in the presence of evolutionary pressure.

# Complex formation of EphA2:Ship2 is influenced by internal dynamics at different temperatures

Dynamic allostery involves changes in fluctuation properties of a residue, domain, or protein without altering the average position of the residue, domain, or protein. Naturally, the dynamics of protein fluctuations should be affected by temperature, perhaps the simplest factor. Our last example examines the general role of a temperature decrease on quenching protein internal dynamics and its influence on protein interactions of representative complex formation of the SAM-bound EphA2:Ship2 heterodimer (denoted E-SAM:S-SAM here) (Lee et al., 2012). This system has moderate binding affinity at the micromolar K<sub>d</sub> level. A drop in temperature is predicted to attenuate, or "quench," many protein fluctuations. To study this effect, we compared the variation of internal protein entropy for the E-SAM:S-SAM association at two different temperatures (300 K and 290 K; Figure 3A). All-atom MD simulations were run for this system at the two temperatures separately with 4 replicates, totaling 12  $\mu$ s (Table S1). The decrease in temperature leads to overall attenuation of amino acid fluctuations; i.e., repression of the RMSFs of amino acids (Figure 3B). This is seen mostly for residues 917–920 at the  $\alpha 1/\alpha 2$  loop, residues 948–951 at the







**DISCUSSION** 

 $\alpha 4/\alpha 5$  loop (/4), and residues 961–966 at  $\alpha 5$  for E-SAM (Figures 3B and 3C). For S-SAM, fluctuation of residues at or next to  $\alpha$ 3 (res. 1222-1229) is heavily repressed. The dynamics of residues of  $\alpha$ 4 and  $\alpha$ 5 are also partially repressed (Figures 3B and 3C). Similar to the case of K-Ras4B, the dynamics of several flexible regions are susceptible to fluctuation repression. Our previous studies have shown that the dimeric interface between E-SAM and S-SAM is largely maintained by native contacts between E-SAM res. 952–957 (/4 and  $\alpha$  4) and S-SAM res. 1220–1224, 1227, and 1235 ( $\alpha$ 3 and  $\alpha$ 4). For E-SAM and S-SAM, many of these residues that experience the largest repression of dynamic fluctuations are at or next to the E-SAM:S-SAM dimeric interfaces. Attenuation of residue fluctuations at low temperatures would diminish the loss of entropy that is needed for formation of the E-SAM:S-SAM dimer.

We calculated the entropy of each SAM domain in the free and complexed proteins from the trajectories as described in the STAR Methods. Full results for entropy values of E-SAM and S-SAM at different time intervals and different replicas are listed in Table S4. The mean entropy values of E-SAM and S-SAM are summarized in Figure 3D. At T = 300 K, the penalty due to the entropy decrease on SAM domain association. -TΔS, is 54.0 kcal/ mol. The entropy penalty at a lower temperature of 290 K is 37.7 kcal/mol. Therefore, at the lower temperature, reduced protein flexibility goes hand in hand with a diminished requirement for a change in internal dynamics upon binding and results in a reduced entropy penalty for protein association. This lesser entropy penalty at low temperature is typically counteracted by an increase in protein-water interactions, increasing the enthalpy penalties for removing water from the protein-protein interaction surfaces (Li and Buck, 2019). Globally, the equilibrium of proteins in bound and unbound states depends on the free energy difference between the two states ( $e^{-\Delta G/kT}$ ). Therefore, if  $\Delta$  G < 0, then a drop in temperature would typically favor the protein-bound state, and the reduced need of entropy penalty is a major source for enhanced association.

In summary, we show examples of how protein or ligand binding, site mutation, and temperature alter the local fluctuation of residues or the plasticity of a domain or a protein without changing the average position or average conformation. These dynamic changes without structural change affect molecular interactions with consequences that likely propagate to successive protein interactions in signaling or other multiprotein events. Dynamics change driven protein interaction (DCDPI) effects are significant and likely to be of great consequence in biology.

Figure 4. A schematic model of quenchingstimulated and tempering-repressed protein association

- (A) Quenching-stimulated protein association.
- (B) Tempering-repressed protein association.

Allostery has long been recognized as a means for a protein molecule to communicate between distant portions of its structure to affect the viability and control of functional outcomes. Conformational change

due to ligand binding is a common and well-studied way in which allostery manifests itself. This type of allostery has dominated most of the studies of allosteric effects to date because it can be detected in a straightforward manner. Dynamic allostery, where changes in fluctuations result in an entropy-driven change in protein behavior in the absence of conformational change, was conceptualized decades ago but has remained relatively unobserved because it is not easily detected by comparing crystal structures and is challenging to quantify by NMR or MD simulations. Here we focus on specific examples that illustrate the concept of dynamic allostery as it pertains to ligand binding or protein-protein interactions, which we specifically refer to as DCDPI: dynamics change driven protein interaction.

Using three specific examples, we illustrated different ways in which protein internal dynamics or local fluctuations of amino acid atoms can be altered with functional consequences: protein binding, mutation, and tempering. All three are observed in nature, maintaining functional viability in a manner that we suspect is much more common than previously appreciated. The DCDPI concept is generalized in Figure 4. Ras:Raf dimerization illustrates quenching of protein internal dynamics after initial complex formation, diminishing the entropy penalty for the subsequent dimerization process. Here we quantify the role of dynamic allostery in the Ras dimerization process as a result of effector (RBD) binding without a conformational change. Dimerization, in turn, has been proposed as a key step in forming an effective mitogen-activated protein kinase (MAPK) signaling platform that may also include scaffold proteins (Packer et al., 2021). Although this example ideally illustrates a dominant entropic effect of protein or ligand binding that promotes further protein association, it is likely that this dynamic allostery effect is present to varying extents, even in cases where conformational change also plays a role. The ADK example illustrates a process that is likely prominent during evolution, with mutations used to compensate for changes in protein fluctuations as a result of environmental variables, such as adaptation to changes in temperature or pressure for maintenance of motion essential for enzyme catalysis (Henzler-Wildman et al., 2007). Finally, the principle of quenching or tempering of internal protein dynamics was explored for complex formation of EphA2:Ship2 at two different temperatures, again illustrating the decrease in entropic penalty because of complex formation as a result of decreased thermal motion in a reduced-temperature environment. For the EphA2:Ship2 simulation, we used the TIP3P water model. The water model may have an influence on the behavior of protein fluctuations at different temperatures. Calculation with different water

# **Theory**



models could provide additional evidence of the dynamics effect, but these calculations go beyond the scope of the present study and could be explored in the future. Overall, the EphA2:Ship2 example makes clear the importance of maintaining homeostasis, balanching perturbations in the finely tuned ensemble of protein fluctuations and the stability of the protein-protein interaction due to changes in temperature. The latter has the potential to substantially disrupt physiological processes as these typically depend on precise protein-protein interaction affinities.

In general, the merit of dynamic-allostery-driven protein association (DCDPI) is simple, but it has been hard to assess because of the difficulty of finding suitable examples of protein associations, which are predominantly driven by the entropy effect. An accurate estimation of protein entropy changes is difficult to obtain from NMR relaxation, chemical shift perturbations, or dynamics simulation trajectories. In the experimentally validated systems that show predominantly dynamic allostery (and little/negligible conformational change), the phenomenon was mostly observed for the cooperative (or negative cooperative) association between protein and two successive binding ions or small molecules. Although we clearly demonstrated the principle of dynamic-allostery-driven protein:protein association using thermodynamics calculations based on simulation methods, it will be important for it to be validated by NMR or other residue-based dynamics experiments. For the RAS:RBD system, ideally one would build a controllable and symmetric system, as we did in the simulation

RAS → RAS:RAS (process I) and

# RBD-RAS → RBD-RAS:RAS-RBD (process II).

Our simulations indicate that changes in entropy in the RBD make a relatively minor contribution to the entropy difference between process I and process II. Thus, isotope labeling and NMR relaxation measurements could be applied to RAS alone. To symmetrically and quantitatively compare process I and process II, proteins must be in monomeric or dimeric states. It is relatively easy to measure the chemical shift for monomeric RAS and monomeric RBD-RAS (by applying a low sample concentration). It would be challenging to measure the chemical shift changes for the RAS:RAS dimer and RBD-RAS:RAS-RBD dimerization because RAS has a weak propensity to form a stable dimer (especially without the RBD) under experimental solution conditions, and it may be difficult to reach saturation (100% of dimer complex formed). A compromise method might involve fusion of two RAS via the long and flexible linker attached to the C-terminal region of the first protein. This dramatically increases the local concentration of RAS to help it form a dimer. Assuming that it would have a minor effect on the intrinsic RAS dimerization interface, this would give dynamics information on dimeric RAS or RBD-RAS. We expect that future experiments will validate this phenomenon.

Despite the challenges of quantifying the entropy changes associated with the process of dynamic allostery, it is important to recognize dynamic allostery as a common aspect of biological processes. Changes in long-range protein fluctuations due to an external stimulus are likely to occur frequently and to have a pivotal role in regulating the subsequent interactions of a protein, affecting its signaling, or a catalytic process. A classic example is the GPCR group of proteins, which, upon agonist stimulation, show an obvious displacement of transmembrane helix 6 (Wootten et al., 2018). The local fluctuations of atoms at the intracellular region could also be changed, but they are essentially regarded as "invisible"/difficult-to-interpret dynamic changes, although sometimes hinted at by crystallographic temperature or B-factors in the structure determination. These changes in dynamics may act alongside the helix 6 conformational change in regulating G-protein binding and, thus, should be analyzed as much as possible (Okude et al., 2015). We expect that, in many systems, especially in weak protein binding systems, the entropy change (quenching or tempering of protein dynamics) has a significant influence, making it as important as a visible structural change in the protein interaction or signaling process. These factors should be characterized further and quantified for more systems in future studies. The calculations provided here provide an important theoretical framework to motivate experiments to establish DCDPI as a common phenomenon guiding biological interactions and functions.

#### **STAR**\*METHODS

Detailed methods are provided in the online version of this paper and include the following:

- KEY RESOURCES TABLE
- RESOURCE AVAILABILITY
  - Lead contact
  - Materials availability
  - Data and code availability
- EXPERIMENTAL MODEL AND SUBJECT DETAILS
- METHOD DETAILS
  - System preparation
  - O General simulation condition
  - Analysis
- QUALIFICATION AND STATISTICAL ANALYSIS

# SUPPLEMENTAL INFORMATION

Supplemental information can be found online at https://doi.org/10.1016/j.str. 2022.03.008.

#### **ACKNOWLEDGMENTS**

We thank the NSF for grant MCB-2121426 (to C.M.) for work on the dimeric Ras protein and information on C-Raf RBD-stimulus Ras dimerization. This work is supported by an NIH R01 grant from the National Eye Institute (R01EY029169) and previous grants from NIGMS (R01GM073071 and R01GM092851) to the Buck lab. Computational resources are partially supported by Advanced Research Computing at Case Western Reserve University. Anton Computer time was provided by the Pittsburgh Supercomputing Center (PSC) through grant R01GM116961 from the National Institutes of Health.

## **AUTHORS CONTRIBUTIONS**

Z.-I.L. and M.B. designed the studies and interpreted the data. Z.-I.L., C.M., and M.B. wrote the manuscript. Z.-I.L. set up, performed, and analyzed the molecular dynamics simulations.

#### **DECLARATION OF INTERESTS**

The authors declare no competing interests.

Received: August 9, 2021 Revised: January 8, 2022 Accepted: March 10, 2022 Published: April 4, 2022





#### REFERENCES

Ahuja, L.G., Aoto, P.C., Kornev, A.P., Veglia, G., and Taylor, S.S. (2019). Dynamic allostery-based molecular workings of kinase:peptide complexes. Proc. Natl. Acad. Sci. U S A *116*, 15052–15061.

Akke, M., Bruschweiler, R., and Palmer, A.G., 3rd (1993a). NMR order parameters and free energy: an analytical approach and its application to cooperative Ca2+ binding by calbindin D9k. J. Am. Chem. Soc. *115*, 9832–9833.

Akke, M., Skelton, N.J., Kordel, J., Palmer, A.G., 3rd, and Chazin, W.J. (1993b). Effects of ion binding on the backbone dynamics of calbindin D9k determined by 15N NMR relaxation. Biochemistry *32*, 9832–9844.

Amaral, M., Kokh, D.B., Bomke, J., Wegener, A., Buchstaller, H.P., Eggenweiler, H.M., Matias, P., Sirrenberg, C., Wade, R.C., and Frech, M. (2017). Protein conformational flexibility modulates kinetics and thermodynamics of drug binding. Nat. Commun. *8*, 2276.

Andricioaei, I., and Karplus, M. (2001). On the calculation of entropy from covariance matrices of the atomic fluctuations. J. Phys. Chem. *115*, 6289–6292.

Arora, K., and Brooks, C.L., 3rd (2007). Large-scale allosteric conformational transitions of adenylate kinase appear to involve a population-shift mechanism. Proc. Natl. Acad. Sci. U S A. *104*, 18496–18501.

Barman, A., and Hamelberg, D. (2016). Coupled dynamics and entropic contribution to the allosteric mechanism of Pin1. J. Phys. Chem. B 120, 8405–8415.

Bouguet-Bonnet, S., and Buck, M. (2008). Compensatory and long-range changes in picosecond-nanosecond main-chain dynamics upon complex formation: 15N relaxation analysis of the free and bound states of the ubiquitin-like domain of human plexin-B1 and the small GTPase Rac1. J. Mol. Biol. 377, 1474–1487.

Chakrabarti, M., Gabelli, S.B., and Amzel, L.M. (2020). Allosteric activation of PI3Kalpha results in dynamic access to catalytically competent conformations. Structure 28, 465–474.e465.

Chung, J.K., Lee, Y.K., Denson, J.P., Gillette, W.K., Alvarez, S., Stephen, A.G., and Groves, J.T. (2018). K-Ras4B remains monomeric on membranes over a wide range of surface densities and lipid compositions. Biophys. J. 114, 137–145.

Cookis, T., and Mattos, C. (2021). Crystal structure reveals the full Ras-Raf interface and advances mechanistic understanding of Raf activation. Biomolecules 11, 996.

Cooper, A., and Dryden, D.T. (1984). Allostery without conformational change. a plausible model. Eur. Biophys. J. 11, 103–109.

Feng, C., Roy, A., and Post, C.B. (2018). Entropic allostery dominates the phosphorylation-dependent regulation of Syk tyrosine kinase release from immunoreceptor tyrosine-based activation motifs. Protein Sci *27*, 1780–1796.

Fetics, S.K., Guterres, H., Kearney, B.M., Buhrman, G., Ma, B., Nussinov, R., and Mattos, C. (2015). Allosteric effects of the oncogenic RasQ61L mutant on Raf-RBD. Structure 23, 505–516.

Grutsch, S., Bruschweiler, S., and Tollinger, M. (2016). NMR methods to study dynamic allostery. PLoS Comput. Biol *12*, e1004620.

Henzler-Wildman, K.A., Lei, M., Thai, V., Kerns, S.J., Karplus, M., and Kern, D. (2007). A hierarchy of timescales in protein dynamics is linked to enzyme catalysis. Nature *450*, 913–916.

Huang, J., Rauscher, S., Nawrocki, G., Ran, T., Feig, M., de Groot, B.L., Grubmuller, H., and MacKerell, A.D., Jr. (2017). CHARMM36m: an improved force field for folded and intrinsically disordered proteins. Nat. Methods *14*, 71–73.

Kaplan, M., Narasimhan, S., de Heus, C., Mance, D., van Doorn, S., Houben, K., Popov-Celeketic, D., Damman, R., Katrukha, E.A., Jain, P., et al. (2016). EGFR dynamics change during activation in native membranes as revealed by NMR. Cell *167*, 1241–1251.e1211.

Koss, H., Bunney, T.D., Esposito, D., Martins, M., Katan, M., and Driscoll, P.C. (2018). Dynamic allostery in PLCgamma1 and its modulation by a cancer mutation revealed by MD simulation and NMR. Biophys. J. *115*, 31–45.

Kovrigina, E.A., Galiakhmetov, A.R., and Kovrigin, E.L. (2015). The Ras G domain lacks the intrinsic propensity to form dimers. Biophys. J. *109*, 1000–1008.

Lee, H.J., Hota, P.K., Chugha, P., Guo, H., Miao, H., Zhang, L., Kim, S.J., Stetzik, L., Wang, B.C., and Buck, M. (2012). NMR structure of a heterodimeric

SAM:SAM complex: characterization and manipulation of EphA2 binding reveal new cellular functions of SHIP2. Structure 20, 41–55.

Li, Z.L., and Buck, M. (2019). Modified potential functions result in enhanced predictions of a protein complex by all-atom molecular dynamics simulations, confirming a stepwise association process for native protein-protein interactions. J. Chem. Theor. Comput *15*, 4318–4331.

Lisi, G.P., and Loria, J.P. (2017). Allostery in enzyme catalysis. Curr. Opin. Struct. Biol. 47, 123–130.

Okude, J., Ueda, T., Kofuku, Y., Sato, M., Nobuyama, N., Kondo, K., Shiraishi, Y., Mizumura, T., Onishi, K., Natsume, M., et al. (2015). Identification of a conformational equilibrium that determines the efficacy and functional selectivity of the μ-opioid receptor. Angew. Chem. Int. Ed. Engl. *54*, 15771–15776.

Packer, M.R., Parker, J.A., Chung, J.K., Li, Z., Lee, Y.K., Cookis, T., Guterres, H., Alvarez, S., Hossain, M.A., Donnelly, D.P., et al. (2021). Raf promotes dimerization of the Ras G-domain with increased allosteric connections. Proc. Natl. Acad. Sci. U S A *118*, e2015648118.

Papaleo, E., Tiberti, M., Invernizzi, G., Pasi, M., and Ranzani, V. (2011). Molecular determinants of enzyme cold adaptation: comparative structural and computational studies of cold- and warm-adapted enzymes. Curr. Protein Pept. Sci. 12, 657–683.

Petit, C.M., Zhang, J., Sapienza, P.J., Fuentes, E.J., and Lee, A.L. (2009). Hidden dynamic allostery in a PDZ domain. Proc. Natl. Acad. Sci. U S A 106, 18249–18254.

Phillips, J.C., Braun, R., Wang, W., Gumbart, J., Tajkhorshid, E., Villa, E., Chipot, C., Skeel, R.D., Kale, L., and Schulten, K. (2005). Scalable molecular dynamics with NAMD. J. Comput. Chem. *26*, 1781–1802.

Popovych, N., Sun, S., Ebright, R.H., and Kalodimos, C.G. (2006). Dynamically driven protein allostery. Nat. Struct. Mol. Biol. *13*, 831–838.

Ranade, S.S., Syeda, R., and Patapoutian, A. (2015). Mechanically activated ion channels. Neuron 87, 1162–1179.

Saavedra, H.G., Wrabl, J.O., Anderson, J.A., Li, J., and Hilser, V.J. (2018). Dynamic allostery can drive cold adaptation in enzymes. Nature 558, 324–328.

Seeber, M., Felline, A., Raimondi, F., Muff, S., Friedman, R., Rao, F., Caflisch, A., and Fanelli, F. (2011). Wordom: a user-friendly program for the analysis of molecular structures, trajectories, and free energy surfaces. J. Comput. Chem. *32*, 1183–1194.

Shaw, D.E., Grossman, J.P., Bank, J.A., Batson, B., Butts, J.A., Chao, J.C., Deneroff, M.M., Dror, R.O., Even, A., Fenton, C.H., et al. (2014). Anton 2: Raising the Bar for Performance and Programmability in a Special-Purpose Molecular Dynamics Supercomputer (IEEE).

Strotz, D., Orts, J., Kadavath, H., Friedmann, M., Ghosh, D., Olsson, S., Chi, C.N., Pokharna, A., Guntert, P., Vogeli, B., et al. (2020). Protein allostery at atomic resolution. Angew. Chem. Int. Ed. Engl. *59*, 22132–22139.

Tzeng, S.R., and Kalodimos, C.G. (2009). Dynamic activation of an allosteric regulatory protein. Nature *462*, 368–372.

Weinkam, P., Chen, Y.C., Pons, J., and Sali, A. (2013). Impact of mutations on the allosteric conformational equilibrium. J. Mol. Biol. *425*, 647–661.

Wootten, D., Christopoulos, A., Marti-Solano, M., Babu, M.M., and Sexton, P.M. (2018). Mechanisms of signalling and biased agonism in G protein-coupled receptors. Nat. Rev. Mol. Cell Biol. *19*, 638–653.

Zerbetto, M., Anderson, R., Bouguet-Bonnet, S., Rech, M., Zhang, L., Meirovitch, E., Polimeno, A., and Buck, M. (2013). Analysis of 15N-1H NMR relaxation in proteins by a combined experimental and molecular dynamics simulation approach: picosecond-nanosecond dynamics of the Rho GTPase binding domain of plexin-B1 in the dimeric state indicates allosteric pathways. J. Phys. Chem. B *117*, 174–184.

Zhang, L., Bouguet-Bonnet, S., and Buck, M. (2012). Combining NMR and molecular dynamics studies for insights into the allostery of small GTPase-protein interactions. Methods Mol. Biol. 796, 235–259.

Zhang, L., and Buck, M. (2017). Molecular dynamics simulations reveal isoform specific contact dynamics between the plexin Rho GTPase binding domain (RBD) and small Rho GTPases Rac1 and Rnd1. J. Phys. Chem. B *121*, 1485–1498





# **STAR**\*METHODS

#### **KEY RESOURCES TABLE**

REAGENT or RESOURCE	SOURCE	INDENTIFIER
Deposited data		
K-Ras4B-RBD	RCSB	PDB: 4DSO, 4G0N, 6W4E
Adenylate kinase	RCSB	PDB: 4AKE
EphA2 SAM: SHIP SAM	RCSB	PDB: 2KSO
Software and algorithms		
NAMD 2.10	Dr. Klaus Schulten, University of Illinois Urbana-Champaign (free software and publically available)	http://www.ks.uiuc.edu/Research/namd
VMD	Dr. Klaus Schulten, University of Illinois Urbana-Champaign (free software and publically available)	http://www.ks.uiuc.edu/Research/vmd/current/node233.html
Python 3.4	Python package	https://www.python.org/download/ releases/3.4.0/
Wordom	Dr. Amedeo Caflisch, University of Zurich & Dr. Francesca Fanelli, University of Modena and Reggio Emilia	http://wordom.sourceforge.net

## **RESOURCE AVAILABILITY**

#### **Lead contact**

Further information and requests for resources should be directed to and will be fulfilled by the lead contact, Matthias Buck (Matthias. Buck@case.edu).

## **Materials availability**

This study did not generate new unique reagents.

# **Data and code availability**

This paper analyzes existing, publicly available protein structures. The accession numbers for the datasets are listed in the key resources table. Molecular dynamics trajectories reported in this paper will be shared by the lead contact upon request. The paper does not report original code. Any additional information required to reanalyze the data reported in this paper is available from the lead contact upon request.

## **EXPERIMENTAL MODEL AND SUBJECT DETAILS**

All data are generated from the datasets provided in the KRT.

#### **METHOD DETAILS**

# **System preparation**

We performed molecular dynamics simulations to study the influence of protein dynamics on protein interaction. We simulated monomeric K-Ras4B (PDB 4DSO) and dimeric K-Ras4B, as well as K-Ras4B in complex with C-Raf RBD and a 2:2 RBD: K-Ras4B: K-Ras4B: RBD complex in solution. The starting structure of K-Ras4B was based on PDB 4DSO. PDB 4G0N was used as a template to model the K-Ras4B: RBD binding interfaces. By contrast to this interaction, due to the weak binding properties, the characterization of Ras dimeric interface has been challenging for years. We used the NMR-driven model of K-Ras4B-GTP homodimer, PDB 6W4E as a template to build the dimeric interface for K-Ras4B (with helices  $\alpha$  4,  $\alpha$  5 at interface). The 2:2 RBD: K-Ras4B: K-Ras4B: RBD system was built first. All the other systems (K-Ras4B, RBD: K-Ras4B or K-Ras4B: K-Ras4B) were extracted from the 2:2 dimeric system and subjected for dynamics simulation. Each simulation was performed for 500 ns. Six and four repeat simulations were performed for dimeric K-Ras4B: K-Ras4B and RBD: K-Ras4B: K-Ras4B: RBD system respectively, starting with different velocity assignments. The K-Ras4B dimer (without RBD) in solution is particularly weak, and has a tendency to dissociate even in short simulations. Thus, two extra simulations were performed for dimeric K-Ras4B to increase the sampling. Since each homodimer system contains duplicated K-Ras4B or RBD, so two values were obtained when we calculated the entropy





for each protein. The two K-Ras4B in K-Ras4B homodimer and the two RBD: K-Ras4B in homodimeric RBD: K-Ras4B were separately extracted from the dimeric conformation and subjected to simulations at same condition. Totally, eight repeat simulations were performed for the monomeric systems (K-Ras4B and RBD: K-Ras4B system).

For Adenylate kinase (ADK), we carried out simulations for wild ADK (PDB 4AKE) and four ADK mutants (A37G, A55G, V135G and V142G respectively) in their inactive open state. Alanine or valine at sites 37, 55, 135, 142 was replaced with Glycine with VMD. Simulations were performed in duplicate for 500 ns for ADK and ADK mutants.

We performed molecular dynamics simulation for monomeric EphA2 SAM (E-SAM) and Ship2 SAM (S-SAM) and heterodimeric EphA2 SAM: Ship2 SAM domain complex at two different temperatures of 300 K and 290 K. Initial protein complex structure was taken from our previous results, which corresponds to the dominant configuration of the SAM: SAM dimer (Lee et al., 2012; Li and Buck, 2019). Free EphA2 SAM or Ship2 SAM domain was obtained by extracting either EphA2 SAM or SHIP2 SAM from the dimeric EphA2 SAM: Ship2 SAM complex. Simulations for this system were run in quadruplicates for 500 ns at the two temperatures.

#### **General simulation condition**

All simulations systems are given in Table S1 in the Supplementary Materials. The proteins were solvated by TIP3P water with 150 mM NaCl; all initial equilibrium simulations were performed with the NAMD/2.12 package (Phillips et al., 2005). A time step of 2 fs was employed. The SHAKE algorithm was applied for all covalent bonds to hydrogen. A Langevin thermostat of 310 K for was used for all simulations, except for EphA2: Ship2 simulations which were at 290K and 300K. A semi-isotropic Langevin scheme at 1 bar were used for pressure control. The van der Waals (vdW) potential was cut off at 12 Å and smoothly shifted to zero between 10 and 12 Å. The long-range electrostatic interactions were calculated with the Particle-Mesh Ewald (PME) method. Production simulations were performed on the Anton 2 supercomputer specialized for MD simulation (Shaw et al., 2014). The CHAMRM36m force field was used in all simulations (Huang et al., 2017). In addition to the simulations described above, in order to gain extra evidence for dynamic allostery-driven Ras association, we performed two short simulation sets each of 200 ns for RBD: K-Ras4B systems, at same simulation condition but with a different force field, i.e, Amber force field (ff19SB).

#### **Analysis**

Root means squared fluctuation (RMSF), clustering, principal mode analysis, and dynamic network analysis was carried out with standard scripts in VMD. The conformational entropy of the proteins was calculated with the quasi-harmonic approximation method (Andricioaei and Karplus, 2001), as implemented in Wordom (Seeber et al., 2011). The precise estimation of absolute entropy of a protein is still challenging in computational modeling. As noted in the study of Amaral et al., the quasi-harmonic approximation method estimates the upper limit of protein conformational entropy and typically overestimates the entropy value by 2-fold or more (Amaral et al., 2017). Since only entropy changes are considered in this paper (eg., entropy of K-Ras in a monomeric form versus entropy of K-Ras in a dimeric form, each with/without RBD binding), this overestimation should mainly affect the absolute value but not the qualitative trends. Non-hydrogen atoms were selected for entropy estimation.

### **QUALIFICATION AND STATISTICAL ANALYSIS**

Data statistical analysis was performed using Python (version 3.4). A two-tailed test was performed to determine statistical difference between mean value of entropy in Figures 1B and 3D. If a p-value is less than 0.05, the result is statistically significant. If a p-value is greater than 0.05, then the result is not significant. For entropy analysis, simulations were performed with multiple repeats (n = 4 for RAS-RBD simulations, and n = 2 for SAM-SAM simulations) and the simulation trajectories were saved at every 10 ps. Trajectory blocks between intervals 100-200ns, 200-300ns, 300-400ns, 400-500 ns were used for entropy calculation. Mean value (S<sub>AVF</sub>) and standard deviation (STD) of entropy were averaged over different trajectories intervals and different repeat simulations. The list of entropy values, the average S<sub>AVE</sub> and the standard deviations is detailed in Table S2 and Table S4.